Thermalization processes in interacting Anderson insulators

Z. Ovadyahu
Racah Institute of Physics, The Hebrew University, Jerusalem 91904, Israel
(Received 11 December 2014; published 13 January 2015)

This paper describes experiments utilizing a unique property of electron glasses to gain information on the fundamental nature of the interacting Anderson-localized phase. The methodology is based on measuring the energy absorbed by the electronic system from alternating electromagnetic fields as a function of their frequency. Experiments on three-dimensional (3D) amorphous indium-oxide films suggest that, in the strongly localized regime, the energy spectrum is discrete and inelastic electron-electron events are strongly suppressed. These results imply that, at low temperatures, electron thermalization *and* finite conductivity depend on coupling to the phonon bath. The situation is different for samples nearing the metal-insulator transition; in insulating samples that are close to the mobility edge, energy absorption persists to much higher frequencies. Comparing these results with previously studied 2D samples [Ovadyahu, Phys. Rev. Lett. **108**, 156602 (2012)] demonstrates that the mean-level spacing (on a single-particle basis) is not the only relevant scale in this problem. The possibility of delocalization by many-body effects and the relevance of a nearby mobility edge (which may be a many-body edge) are discussed.

DOI: 10.1103/PhysRevB.91.035113 PACS number(s): 72.80.Ng, 73.61.Jc, 72.20.Ee

I. INTRODUCTION

The question of how Coulomb interactions affect Anderson localization has been a challenging problem for decades. It was first addressed by Fleishman and Anderson [1] in the context of the stability of the insulating phase as well as the mechanism of system thermalization and energy exchange involved in hopping conductivity. Thermalization of Fermi-gas systems depends on inelastic scatterings of electrons. Energy exchange via electron-electron (*e-e*) scattering is required for establishing the Fermi-Dirac thermal distribution, which defines the electron temperature. Such events lead to decoherence of the electrons and thus also control the quantum effects exhibited by the system.

The most frequently encountered mechanisms for electronic energy-transfer in condensed matter systems are e-e and electron-phonon (e-ph) scatterings. The latter is needed to maintain steady-state conditions when the system is driven by an external source, and in particular, is responsible for the validity of Ohm's law.

In metallic systems at sufficiently low temperatures the e-e inelastic rate $\gamma_{in}^{e\text{-}e}$ is usually the main source of scattering [2]. Both $\gamma_{in}^{e\text{-}e}$ and the e-ph inelastic rate $\gamma_{in}^{e\text{-}ph}$ can be measured in the diffusive regime based on weak-localization effects [3]. While similar quantum effects sometime extend into the hopping regime of the same system [4], a theoretical framework to analyze such data and obtain inelastic scattering rates is unfortunately not yet established. $\gamma_{in}^{e\text{-}e}$ in the hopping regime is defined in this work as the rate of energy exchange δE involved in electron-electron scatterings where $\delta E \neq 0$. These processes contribute to the *overall* lifetime broadening of the electronic level, which is what our experiments are designed to capture. It should be remarked that the energy-state broadening includes the contribution of other mechanisms (such as electron-phonon inelastic scattering). In the diffusive regime the contribution of e-e inelastic rate may be separated from the e-ph one as demonstrated by Bergmann [3]. This is not yet achievable by the methodology used here for the insulating regime. On the other hand, this method yields information on a wide frequency range (rather than just an average value for the inelastic rate) and it can still be shown that relative to the diffusive regime $\gamma_{in}^{e\text{-}e}$ is dramatically suppressed.

It was recently shown that in the two-dimensional (2D) hopping regime of crystalline indium-oxide $In_2O_{3\text{-}x}$, $\gamma_{in}^{e\text{-}e}$ is suppressed by ≈six orders of magnitude relative to its value at the diffusive regime at the same temperature [5]. This was based on utilizing a unique property of electron glasses [6]; using a non-Ohmic field to take the system out of equilibrium, it endows the system with excess conductance that may be used as an empirical measure of the energy absorbed by the electrons from the field. This technique allows a measurement on systems with very small volume, it is sensitive enough to allow for weak absorption from electric fields, and can be carried over a wide frequency range.

Here we report on measurements performed on Anderson-localized amorphous indium-oxide films (In_xO) that exhibit three-dimensional (3D) hopping transport. The results of our measurements suggest that e-e energy exchange in In_xO is strongly suppressed relative to its value in the diffusive regime at the same temperature. Analysis of these results suggests that thermalization of the electronic system is governed by $\gamma_{in}^{e\text{-}ph}$ as was the case in the 2D crystalline version [5]. However, approaching the metal-insulator transition by reducing the quenched disorder, the perceived inelastic rate tends towards the $\gamma_{in}^{e\text{-}e}$ value typical of the diffusive regime. This occurs while the system is still insulating; it exhibits variable-range-hopping transport and its disorder is as strong as that of the 2D samples where $\gamma_{in}^{e\text{-}e}$ was highly suppressed [5]. We point out some similarity of these observations with a peculiar temperature dependence of the conductivity in 3D systems near their metal-insulator transition, which has been observed in several materials. The role of dimensionality, inherent inhomogeneities, many-body effects, and other issues that might be involved in bringing about an apparent delocalized behavior are discussed.

II. EXPERIMENT

A. Samples preparation and characterization

Three batches of In_xO samples were used in this study. They were prepared by e-gun evaporation onto room-temperature substrates using 99.999% pure In_2O_{3-x} sputtering target pieces. Substrates were either 1-mm-thick microscope glass slides, or on 0.5-μm SiO_2 layer thermally grown on ⟨100⟩ silicon wafers. Samples thickness d was 630 or 1050 Å for the glass slides, and $d = 750$ Å for the Si wafers. Rate of deposition and thickness were measured by a quartz thickness monitor calibrated using optical interference measurements on thick MgF_2 films. Deposition was carried out at the ambience of $(1–3)\times 10^{-4}$ Torr oxygen pressure maintained by leaking 99.9% pure O_2 through a needle valve into the vacuum chamber (base pressure $\simeq 10^{-6}$ Torr). Rates of deposition used for the samples reported here were typically 0.6–0.9 Å/s. Under these conditions, the In_xO samples had carrier concentration n in the range $(7–8)\times 10^{19}$ cm^{-3} as measured by Hall effect at room temperatures on samples that were patterned in a six-probe configuration using stainless-steel masks. These samples were prepared during the same deposition as the strips used for the low-temperature transport measurements. A standard Hall-bar geometry was used with the active channel being a strip 1 mm wide and 10 mm long. The two pairs of voltage probes (that doubled as Hall probes), were spaced 3 mm from one another along the strip. This arrangement allowed us to assess the large scale uniformity of the samples, both in terms of the longitudinal conductance and the Hall effect. Excellent uniformity was found on these scales; resistivities of samples separated by 1 mm along the strip were identical to within ±5%. No change (within the experimental error of 3%) was observed in the Hall effect due to annealing (tested for samples with room-temperature resistivity smaller than $\simeq 0.4$ Ω cm which was the highest ρ in the samples studied in this work). On a mesoscopic scales (10–100 nm) however, In_xO films show compositional inhomogeneities; the various effects these may have on transport properties of these films were reported in Ref. [7].

As-deposited samples had room-temperature resistivity ρ in excess of 10^5 Ω cm which, for the low-temperature studies, had to be reduced by several orders of magnitude. This was achieved by thermal annealing at temperatures $T_a < 75\,^\circ$C to prevent crystallization. For a comprehensive description of the annealing process and the associated changes in the material microstructure see [7].

B. Measurements techniques

Conductivity of the samples was measured using a two-terminal ac technique employing a 1211-ITHACO current pre-amplifier and a PAR-124A lock-in amplifier. Except when otherwise noted, measurements reported below were performed with the samples immersed in liquid helium at $T = 4.1$ K maintained by a 100-liter storage dewar. This allowed long-term measurements of samples as well as a convenient way to maintain a stable bath temperature. The ability to keep the sample at ≈4 K for long times is essential for these studies where a typical series of measurements takes 4–6 weeks to accomplish. The ac voltage bias, used during the off-stress periods, was small enough to ensure linear-response conditions (judged by Ohm's law being obeyed within the experimental error).

As a measure of disorder we use the Ioffe-Regel dimensionless parameter, $k_F\ell = (9\pi^4/n)^{1/3}\frac{R_Q}{\rho_{RT}}$ where $R_Q = \hbar/e^2$ is the resistance quantum. This is based on free-electron expressions using the measured room-temperature resistivity ρ_{RT} and the carrier concentration n, obtained from the Hall-effect measurements, as parameters.

Several sources were used for exciting the system by non-Ohmic fields: the internal oscillator of the PAR124A (up to 2 kHz and 10 V rms), Fluke PM5138A (dc and up to 10 MHz and 40 V p.p.), and Tabor WS8101 (up to 100 MHz and boosted, when necessary, by Ophir 5084 rf power amplifier). Complementary studies in the microwave regime employed the high-power synthesizer HP8360B. Care was taken in these experiments to use "rf-safe" components near the sample immediate vicinity to minimize spurious heating. For the same reason, it was ascertained, by performing four-probe measurements, that the contacts resistance was always negligible relative to the sample resistance.

Optical excitation was accomplished by exposing the sample to AlGaAs diode (operating at $\approx 0.88 \pm 0.05$ μm), placed ≈15 mm from the sample. The diode was energized by a computer-controlled Keithley 220 current source. The samples were attached to a probe equipped with calibrated Ge and Pt thermometers and were wired by triply shielded cables to BNC connectors at room temperatures. The effective capacitance of the wires was $\leqslant 20$ pF. This allowed the use of 23–1500-Hz ac technique without a significant phase shift for any of the samples used here.

Fuller details of measurement techniques are given elsewhere [8].

III. RESULTS AND DISCUSSION

A. Absorption measured via nonequilibrium transport

The main technique used in this study is the "stress protocol" previously used in aging experiments [9]. The procedure is composed of the following stages (see Fig. 1 for details): After the sample is equilibrated at the measuring temperature (typically for 24 h), its conductance versus time $G(t)$ is recorded while keeping the electric field F_0 small enough to be as close to the Ohmic regime as possible. This defines a baseline "equilibrium $G(0)$." Next, F is switched to a non-Ohmic "stress field" F_{stress}, which is kept on the sample for a time t_w. Initially, F_{stress} causes the conductance to increase by ΔG, but G is observed to keep increasing slowly throughout t_w. Then the field is switched back to F_0 and the conductance is continued to be measured for a few thousand seconds. This last stage is depicted in Fig. 1 as a relaxation of $G(t)$ towards the equilibrium $G(F_0)$ with a logarithmic law characteristic of the relaxation processes in electron glasses [10]. A measure of the magnitude of the excess conductance that results from the stress is δG_0 (see inset to Fig. 1), defined by extrapolating the $\delta G(t)$ curve to 1 s as illustrated in the inset to Fig. 1. $\delta G(t)$ is $G(F_0,t) - G(F_0)$. The origin of time for the logarithmic plot in the inset is taken as $t_w + 1$ (i.e., 1 s after F_{stress} is reset to the Ohmic field F_0).

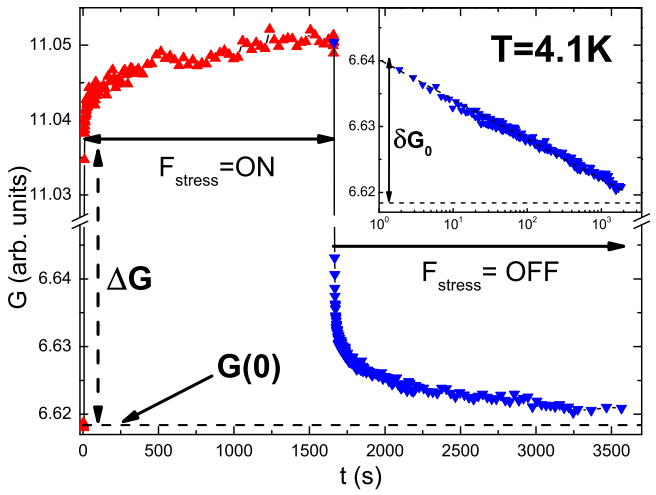

FIG. 1. (Color online) Conductance vs time $G(t)$ illustrating a typical run of a stress protocol. The sample here is an In_xO with $d = 630$ Å and resistivity $\rho = 21.4\ \Omega$ cm at $T = 4.1$ K. The Ohmic and stress fields here are $F_0 = 100$ V/m and $F_{\rm stress} = 10^5$ V/m, both at 73 Hz. The inset shows the logarithmic relaxation of $\delta G(t)$ and the definition of δG_0. Dashed lines delineate the equilibrium conductance $G(F_0)$.

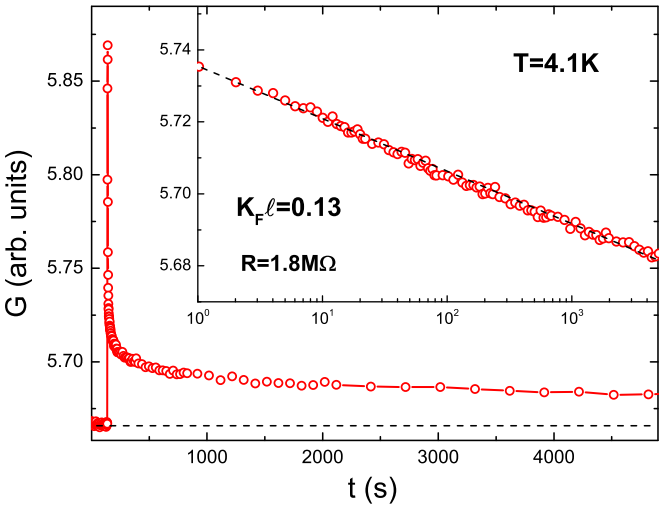

FIG. 2. (Color online) Excitation by IR exposure; after 12 s from start of run, a small IR emitter light-emitting diode (LED) placed $\simeq$1 cm from the sample is energized by a 1-mA current for 3 s then the LED is turned off. $G(t)$, continuously monitored throughout the run, reaches a peak ($\simeq$5.87 on the ordinate) then slowly decays towards its equilibrium value. As in Fig. 1, the ensuing relaxation is logarithmic (inset). Note however, that the initial amplitude for the relaxation falls short of the conductance peak (compare with the gate protocol in Fig. 3). The initial ($<$1 s) fast decay is due to the heating that accompanies the IR radiation. Dashed horizontal line marks the near-equilibrium G.

The relaxation of the excess conductance $\delta G(t)$ is a manifestation of the system approach to equilibrium from an excited state. A negative time derivative of $\delta G(t)$ reflects the energy release to the bath. This energy may have been imparted to the system by a number of different mechanisms; for example, exposing the sample to infrared radiation (Fig. 2), or changing its carrier concentration using a nearby gate (Fig. 3). In either case, the ensuing logarithmic relaxation of δG_0 follows the same relaxation law as that produced by the stress field.

The mechanism by which stressing the system with a non-Ohmic field increases the electronic energy is essentially Joule heating; the energy absorbed by the electrons gives rise to an excess phonons, making it somewhat "hotter" than the bath. A steady state may be established, while the stress field is on, by the flow of energy carried by the phonons in the sample into the thermal bath. The increased density of high-energy phonons (over the phonon population in equilibrium at the bath temperature), randomizes the charge configuration of the electron glass in a similar vein as raising the bath temperature would [11]. This produces the excess conductance that relaxes back to its near equilibrium value once the stress is relieved.

It is therefore plausible to take δG_0 as a measure of the energy $\delta\varepsilon$ absorbed by the electronic system from the field. As long as $\delta G_0/G(0) \ll 1$, δG_0 is arguably proportional to $\delta\varepsilon$.

It is emphasized that the only assumption we make in this procedure is that $\delta\varepsilon$ enters the sample via the coupling of $F_{\rm stress}$ to the *electronic system*. No other assumption is made. In particular, the reason for the very sluggish release of this energy is not relevant for our considerations in this work. The logarithmic nature of $\delta G(t)$ is taken as a convenient empirical fact that allows us to estimate the absorption via transport measurements. This rationale was used in Ref. [5] in the study of the frequency dependence of the electronic absorption of two-dimensional (2D) films of In_2O_{3-x}. In this study we extend the study to three-dimensional (3D) films.

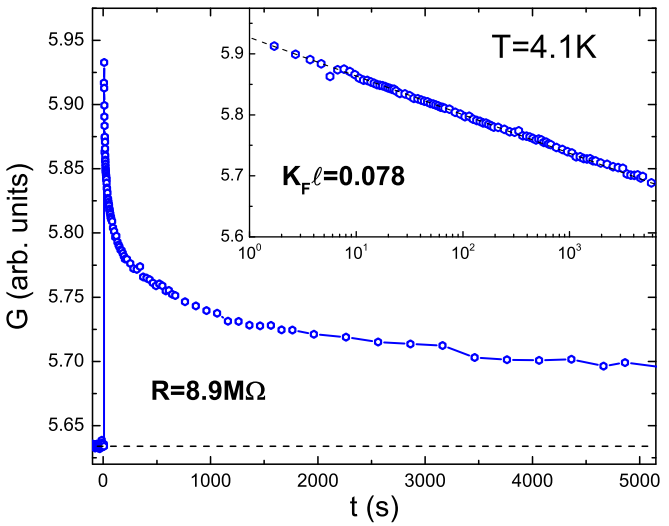

FIG. 3. (Color online) Exciting the sample by the "gate-protocol"; the sample is on a 1-mm-thick glass substrate with a conducting silver-paint coating on its back side acting as gate. After $G(t)$ is monitored for $t = 90$ s to establish a baseline G, the gate voltage, initially at -198 V is switched to $+198$ V in 2 s, and is held there for the remainder of the run. The inset shows that the excess conductance after the switch relaxes logarithmically. Note that the initial amplitude of the relaxation process coincides essentially with the excitation peak.

B. Electronic absorption versus frequency and disorder

Our first goal here is to define a protocol that allows a meaningful comparison between energy absorption from the stress-field applied to the system at various frequencies. The natural choice is to normalize $\delta G_0^{\rm f}$—the excess conductance measured under $F_{\rm stress}$ at a frequency f by $\delta G_0^{\rm dc}$—the excess conductance measured with a dc field while keeping the same $\delta G/G(0)$ and the same $t_{\rm w}$ for each tested frequency of the applied stress. It was found that for $f < 30$ Hz $\delta G_0^{\rm f}$ was indistinguishable (within the experimental error) from $\delta G_0^{\rm dc}$ and in the experiments reported here we used the result for $F_{\rm stress}$ operating at $f = 11$–23 Hz as the normalizing value. For applying the stress protocol at frequencies above $\approx$1 kHz, the conductance was measured at $f = 23$ Hz and under low-bias conditions to ensure linear-regime measurement throughout the protocol. A stress field $F_{\rm stress}$ with frequency f was capacitively superimposed across the sample. The high-frequency component of $F_{\rm stress}$ was filtered out in the input to the current preamplifier (in addition to the band-pass filtering in the 124-A lock-in amplifier) such that the conductance was measured at the low frequency. The amplitude of $F_{\rm stress}$ was adjusted to achieve the desired $\delta G/G(0)$ based on the conductance reading at $f = 23$ Hz. The relaxation part of the protocol was always measured under near-Ohmic conditions and at a low frequency (or at dc).

Results of absorption at different frequencies for three of the 3D samples studied with the protocol described above are shown in Fig. 4. For comparison, the figure includes the 2D samples studied previously [5].

Looking at these data one notes the following:

(1) The general trend is for the absorption to decrease with frequency, and in all three cases shown in Fig. 4 there is a faster decline of the absorption with f above a certain roll-off frequency $f_{\rm RO}$. It is observed that $f_{\rm RO}$ is considerably lower than the respective electron-electron inelastic rate $\gamma_{\rm in}^{\rm e\text{-}e}$ of the material (based on measurements performed on a 3D In_xO system in its diffusive regime at the same temperature).

(2) The frequency range over which the absorption decays appears to be rather wide, extending over several decades. For comparing results under different conditions, we take $f_{\rm RO}$ to be the frequency where $\delta G_0^{\rm f}/\delta G_0^{\rm dc} = 1/2$.

(3) For the range of disorder shown, there seems to be no dependence on the disorder in either three or two dimensions; samples with different disorder show essentially identical absorption versus f curves. However, as will soon transpire, this is only true for samples in the strongly localized regime.

It has been shown [5] that the roll-off frequency in the two-dimensional In_2O_{3-x} samples (lower graph in Fig. 4) is consistent with the electron-phonon inelastic scattering rate $\gamma_{\rm in}^{\rm e\text{-}ph}$ of the material at 4 K. This estimate was based on the assumption that, while under a dc stress field, the system reaches steady-state conditions in which case the energy absorbed by the electrons from $F_{\rm stress}$ equals the energy dissipated into the bath. This may be described by the following expression:

$$\frac{V^2}{R(V)} = C_{\rm el}(T^*)U\Delta T\gamma(T^*). \qquad (1)$$

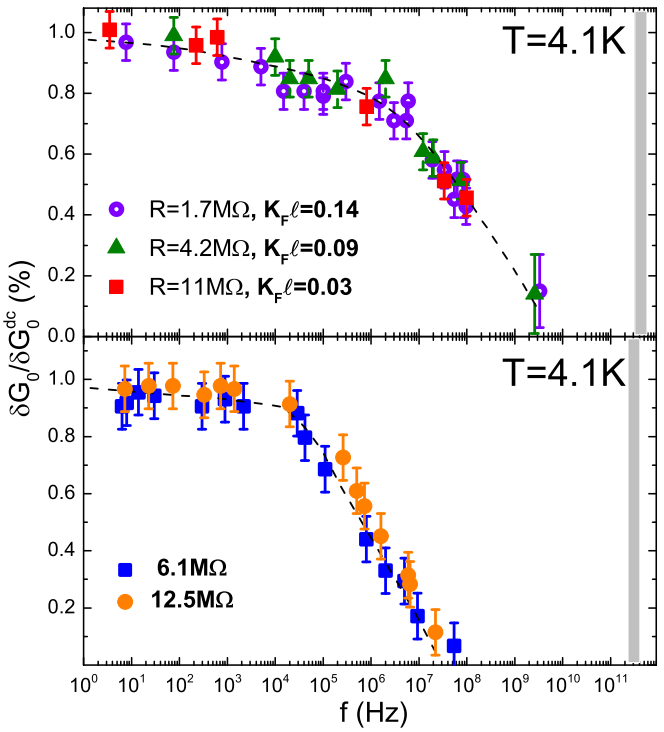

FIG. 4. (Color online) Relative absorption as function of the stress-field frequency for three In_xO samples ($d = 630$ Å for circles and triangles, and $d = 1050$ Å for the squares). These are labeled by their resistance at 4.1 K and their $k_F\ell$ values (top plate). The larger error bars for the $f > 2$-GHz data are based on $F_{\rm stress}$ in the microwave range where $\delta G/G(0)$ was typically limited to $\simeq$0.1 rather than the 0.6 for the smaller frequencies. These results are compared with the data obtained on 2D In_2O_{3-x} films ($d = 52$ Å, taken from [5]). The shaded area marks the respective ranges for $\gamma_{\rm in}^{\rm e\text{-}e}$ of these materials in their diffusive regime at $\simeq$4 K (based on Refs. [7] and [5] for In_xO and In_2O_{3-x} respectively). Dashed lines are guides for the eye.

The left-hand side of Eq. (1) is the Joule-heating term; V is the voltage across the sample, and $R(V)$ is its resistance under V. The right-hand side is the heat-removal rate while $F_{\rm stress}$ is on, and assuming steady-state conditions. In this equation $C_{\rm el}$ is the electronic heat capacity, U is the sample volume, T^* is an "effective electron temperature," ΔT is $T^* - T_{\rm bath}$ (the bath temperature). For our samples being macroscopic, $\gamma(T^*)$ should coincide with the inelastic electron-phonon rate $\gamma_{\rm in}^{\rm e\text{-}ph}$.

The parameters needed for calculating $\gamma(T^*)$ are all obtained from measurements on the respective sample except for $C_{\rm el}$ and T^*. Following the procedure used in Ref. [12], T^* may be estimated from $G(T)$ data (the uncertainty associated with this procedure will be commented on below).

The electronic heat capacity $C_{\rm el}$ is proportional to the temperature and to $\partial n/\partial\mu$, the thermodynamic density of states of the material. Since the carrier concentration of the In_xO samples used in this work is comparable to that of In_2O_{3-x} (and therefore $C_{\rm el}$ for them should be similar), we can estimate the ratio between $\gamma_{\rm in}^{\rm e\text{-}ph}$ of In_xO to that of the In_2O_{3-x} samples by

$$\frac{\gamma_{\rm a}(T^*)}{\gamma_{\rm c}(T^*)} = \frac{V_{\rm a}^2 R_{\rm c}(V_{\rm c})U_{\rm c}\Delta T_{\rm c}}{V_{\rm c}^2 R_{\rm a}(V_{\rm a})U_{\rm a}\Delta T_{\rm a}}, \qquad (2)$$

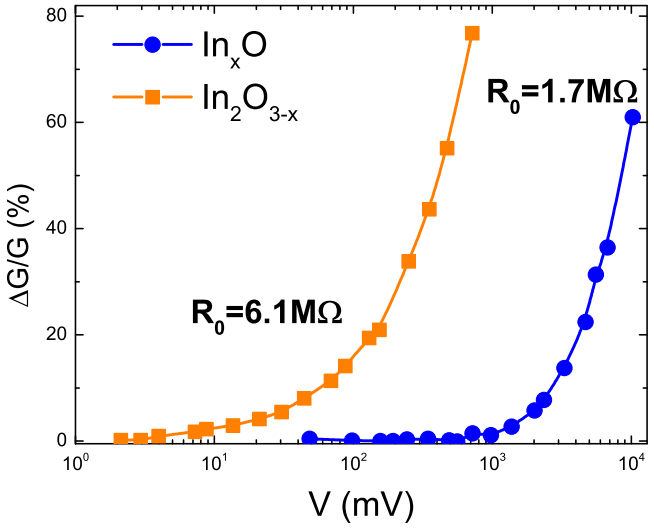

FIG. 5. (Color online) The fractional change of conductance due to applied voltage. The data are for a 2D In_2O_{3-x} film (squares, same sample as in Fig. 4 bottom plate), and a 3D In_xO sample (circles, same as in Fig. 4 top plate).

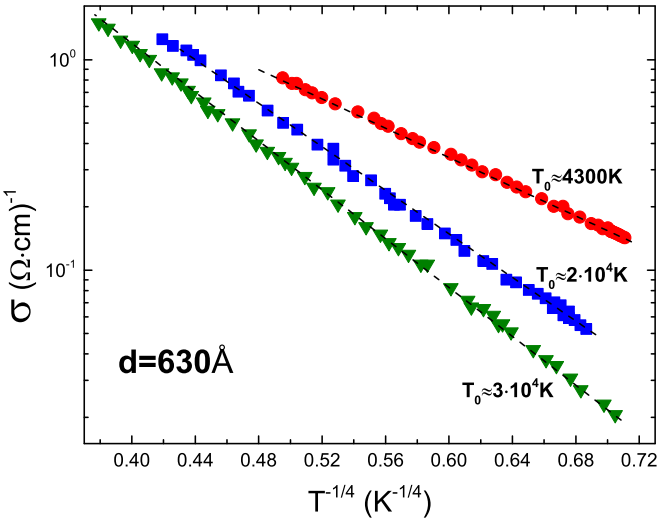

FIG. 6. (Color online) The temperature dependence of conductivity σ for three In_xO samples with different degrees of disorder (obtained by thermal annealing from a single deposition batch). Samples are labeled with their characteristic energy T_0 extracted from the data plotted to conform with $\sigma(T) = \sigma(0)\exp(-[T_0/T]^{1/4})$.

where the subscripts "a" and "c" signify values for the amorphous and crystalline material respectively. The voltages used in the respective experiments are extracted from the conductance-voltage $G(V)$ measurements of the respective samples. For the samples we chose for the analysis below, these data are shown in Fig. 5.

The conditions that were used in the stress protocol for our experiments were $\delta G(0)/G(0) \approx 0.6$, and the associated $F_{\rm stress}$ was applied for $t_w = 1400$ s. To achieve this $\delta G(0)/G(0)$ a voltage of $10.2V = V_a$ was needed for the In_xO sample as compared to $0.5V = V_c$ for the crystalline sample [5], as can be read from Fig. 5. Note that these values (with the respective resistances), mean that the power invested from the (dc) field is ≈1500 times larger for the In_xO sample. The volumes for these samples were 10^{-14} m$^3 = U_c$ and 1.2×10^{-13} m$^3 = U_a$. The "effective temperature" T^* for the In_2O_{3-x} sample estimated in Ref. [5] was 4.8 K $\approx T_c^*$. This was based on the measured $G(T)$ data for the sample under steady-state conditions. Using the same logic here, the respective T^* for the In_xO sample, based on its $G(T)$ data, is 5.3 K $\approx T_a^*$. The conductance versus temperature curves for this sample and two other samples of the same In_xO batch with different degrees of disorder are shown in Fig. 6 below.

It should be remarked that using the sample resistance as a thermometer to obtain T^* is a dubious procedure; in general, the resistance change due to the applied non-Ohmic field is not *just* a heating effect. In fact, deep in the hopping regime *most* of the resistance decrease is actually due to field-assisted hopping [13]. Hopping conductivity may be significantly enhanced by field while a negligible increase of the electrons' "temperature" is observed; application of microwaves for example, may cause a $\delta G > 0$ with essentially no heating [14], and the data in Fig. 4 demonstrate that this adiabatic effect gradually manifests itself even at lower frequencies. In using Eq. (2) for comparing between γ_a and γ_c it is tacitly assumed that the part (reflected in ΔG) due to Joule heating is the same for both materials. The error in the determination of T^* by assuming that G is a faithful thermometer is partially reduced in the ratio $\Delta T_c/\Delta T_a$.

With these reservations, we use the above parameters in Eq. (2) which gives $\gamma_a/\gamma_c = 65$. This value is not far from the factor of ≈75 difference between the roll-off frequencies of the two materials (see Fig. 4), which in view of the uncertainties inherent in the procedure should be judged as a satisfactory agreement.

The larger $\gamma_{\rm in}^{\rm e\text{-}ph}$ of the amorphous material relative to In_2O_{3-x} found in this work is plausible; $\gamma_{\rm in}^{\rm e\text{-}ph} \approx 10^8$ s^{-1} at $T \approx 4$ K is typical of many degenerate Fermi systems [15]. As a rule, phonons in amorphous materials are softer than the crystalline version of the same substance. Soft phonon modes of the amorphous phase usually lead to enhanced electron-phonon coupling. This is probably part of the reason why In_xO, with less disorder and high carrier concentration, is a superconductor below a few K while In_2O_{3-x} remains a normal conductor down to ≈12 mK even when in the metallic regime [16].

As to the second issue listed above, the extended range over which the absorption decreases with frequency, it is especially conspicuous for the In_xO samples. This wide range of $\gamma_{\rm in}^{\rm e\text{-}ph}$, is presumably a consequence of a wide distribution of localization lengths ξ, an inherent property of the disordered system. It is noteworthy that the absorption starts to diminish quickly at a rather small frequency (Fig. 4) suggesting a reduced $\langle\gamma_{\rm in}^{\rm e\text{-}ph}\rangle$. This is not surprising; note that each inelastic scattering of electron by a phonon involves the overlap of an initial state $|i\rangle$ with a final state $|j\rangle$ and a phonon with the energy that matches the energy difference between these sites. Unless compensated somehow by a disorder-enhanced phonon-electron matrix element [17], this inevitably should lead to reduced transition rates relative to the diffusive regime where both states are extended. Unfortunately, there is yet no theory for $\gamma_{\rm in}^{\rm e\text{-}ph}$ in the hopping regime to compare our results with.

C. Reduced decoherence in the insulating regime?

The frequency dependence of the absorption results discussed above suggests that $\gamma_{in}^{e\text{-}e}$ (and, in some sense, also $\gamma_{in}^{e\text{-}ph}$) is suppressed relative to its typical values in the diffusive regime. In the case of $\gamma_{in}^{e\text{-}e}$ this reduction is by several orders of magnitude (see Fig. 4). These rates being the main sources of decoherence in most disordered electronic systems, the following question arises: Does it also mean that there is less decoherence in the Anderson insulator phase?

If one ignores the possibility that the highly disordered phase may breed decoherence agents that were not present in the diffusive regime, like new types of two-level systems or local magnetic moments [18], then the answer is yes; the insulating phase may have reduced inelastic rate relative to the diffusive phase. This however applies to the coherence *time*; the *spatial* extent of the electron coherence will be limited by the highly reduced diffusion constant. There is experimental evidence for quantum coherent effects in the Anderson localized regime that, in some respects, are more prominent than in the diffusive regime but the phase-coherent length is limited to the hopping length [19]. The most compelling evidence for quantum-coherent effects is the anisotropy of conductance fluctuations produced by magnetic field at different orientations is mesoscopic samples as well as in the magnetoresistance of two-dimensional samples [4]. The existence of quantum-coherent effects deep in the hopping regime ought not be surprising. The overlap between the initial and final state is affected by the interference between different spatial trajectories. The phonon involved in the actual transition does not destroy the interference once the phonon wavelength exceeds the hopping length, which inevitably happens at sufficiently low temperatures [4].

The suppression of $\gamma_{in}^{e\text{-}e}$ may appear as a natural consequence of the spectrum discreteness associated with localization [20,21]. On closer examination, and taking into account the role of Coulomb interaction, this issue is more complicated and yet unresolved. The problem was first raised by Fleishman and Anderson [1]. They considered several scenarios by which interactions may modify the single-particle aspects of Anderson-localized systems, while noting that $G(T)$ of these systems still conforms to the variable-range-hopping law. It may be illuminating then to see what we can infer from the VRH conductivity of the samples on the spectrum discreteness.

The space confinement due to localization forces a discrete energy spectrum with a mean level spacing of order (many-body effects may modify this expression [20]):

$$\delta(\xi) \approx (\partial n/\partial\mu\xi^3)^{-1}. \tag{3}$$

To get an estimate of $\delta(\xi)$ one may use data for the temperature dependence of the hopping conductivity. This version of In_xO obeys Mott's law (cf., Fig. 5) $\sigma(T) = \sigma(0)\exp[-(T_0/T)^{1/4}]$ where T_0 is given by [22]

$$k_B T_0 \approx \left(\frac{3}{\partial n/\partial\mu\xi^3}\right). \tag{4}$$

Using the data for $\sigma(T)$ (Fig. 6) and Eq. (4), the mean-level spacing for the two samples studied in Fig. 4 is $\delta(\xi) \approx 10^4$ K $\gg$ 4 K, and it is also much larger than $E_C \approx e^2/(\kappa\xi)$

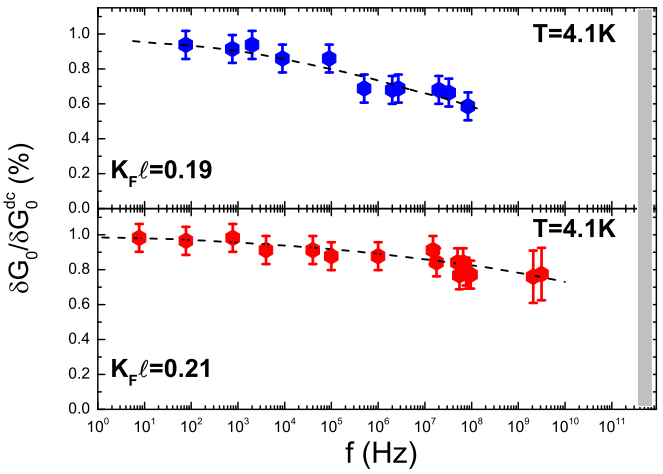

FIG. 7. (Color online) Relative absorption as function of the stress-field frequency for the two In_xO samples that are nearest to the MIT (labeled by their $k_F\ell$ values). The shaded area marks the typical range of $\gamma_{in}^{e\text{-}e}$ of In_xO in its diffusive regime at $\simeq$4 K (based on Ref. [7]). Dashed lines are guides for the eye. Note the difference between these results and the results for the more disordered samples (Fig. 4 top plate),

where $\kappa \simeq 10$ is the dielectric constant for indium-oxide [23], and $\xi \geqslant 10$ Å as will be shown below. Therefore, unless many-body physics plays a role, it would appear that the spectrum discreteness is large enough to suppress electron-electron inelastic scattering. Thermalization of the electronic system and nonzero conductivity then depend on the existence of a continuous bath, presumably phonons. Fleishman and Anderson [1] reached this conclusion for the localized system in the limit of short-range interaction. Our absorption versus frequency results (Fig. 4) are consistent with their conclusions for a realistic interaction range, probably of the order of the hopping length $r(T) \approx \xi(T_0/T)^{1/3}$ or $\approx\xi(T_0/T)^{1/4}$ in two or three dimensions respectively.

The suppression of $\gamma_{in}^{e\text{-}e}$ of Anderson insulators turns out however to be true only for samples in the strongly disordered regime; things appear to be more complicated as the metal-insulator transition (MIT) is approached.

The frequency dependence of the absorption measured on two samples that were annealed to bring their $k_F\ell$ to 0.19 and 0.21 is shown in Fig. 7. These data exhibit a different trend than the more disordered samples shown in Fig. 4 above; the absorption still decreases with frequency but it seems to extend to higher frequencies, possibly even surpassing the $\gamma_{in}^{e\text{-}e}$ of the diffusive regime at this temperature. At the same time, these samples are on the insulating side of the MIT, and their mean-level spacing is still much larger than both E_C and the bath temperature; their characteristic energies T_0 (defined by the VRH conductivity expression) are $\approx$4300 K (Fig. 6) and $\approx$6600 K (Fig. 9 below) for the sample with $k_F\ell = 0.21$ and 0.19 respectively.

More intriguing is the observation that the disorder of the samples in Fig. 4 is considerably larger than that of the 2D samples (Fig. 3 in Ref. [5] and Fig. 4); the disorder in the latter is comparable to that of these 3D samples in terms of $\delta(\xi)$ (and in terms of bulk resistivity the disorder in the 2D films is even *much weaker* than in the 3D samples). If the reason for

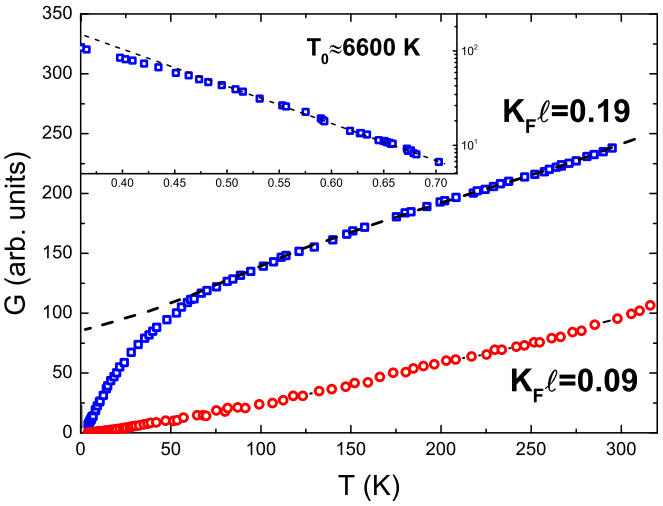

FIG. 8. (Color online) Conductance vs temperature for two of the samples studied for absorption as function of frequency. The sample with $k_F\ell = 0.19$ illustrates the T^* problem—its $G(T)$ data for $T > 60$ K extrapolates to a finite G at $T = 0$ (dashed line). The inset shows that the low-temperature dependence of this sample is variable range hopping. Compare these $G(T)$ data with the data in Fig. 1(b) of [25] and with Fig. 14 of Ref. [24].

the energy-absorption cutoff in the 2D samples is the spectrum discreteness of the electronic states [having $\delta(\xi) \gg k_B T$] then why is the same not sufficient for 3D samples that exhibit equally large $\delta(\xi)$?

D. The "T^* problem"

A possible direction to look for the difference between the 2D and 3D results may be related to the materials; as noted above amorphous and crystalline versions of indium-oxide have their differences but none that seems relevant for this particular feature. On the other hand, there is reason to suspect that *dimensionality* plays a role: Just insulating 3D samples of In_2O_{3-x} exhibit transport peculiarities that are not observed in two dimensions [24]. The 3D samples exhibited insulating characteristics only when cooled below a disorder-dependent T^*. Above this temperature, they show a metalliclike $G(T)$ law. On the other hand, 2D samples of this material with the same range of bulk resistivity exhibited insulating behavior ($\sigma \to 0$ when $T \to 0$) over the same temperature range [24]. Three-dimensional samples of In_xO also exhibited the same "T^* problem" [24]. To illustrate, an example of the T^* problem is shown in Fig. 8 using one of the currently studied specimen. Note that, at low temperatures, $G(T)$ exhibits VRH conductivity (see inset to Fig. 8). This implies $G(T \to 0) = 0$, which means the system is *insulating*. However above $T^* \approx 60$ K the conductance law changes, and if one has no knowledge of the behavior of $G(T)$ at lower temperatures one will conclude, extrapolating along the dashed curve in the main figure that $G(T \to 0) > 0$, that the system is actually a *metal*.

A similar $G(T)$ anomaly appears in quite a few other 3D systems [note that this feature is easier to identify when $G(T)$ rather than $R(T)$ is plotted]. Such a peculiar $G(T)$ may be seen in a series of amorphous $Mn_x Si_{1-x}$ samples [25], in amorphous $Si_{1-x} Cr_x$ [26], in GeAl [27], in granular aluminum [24], in crystalline $GeSb_2Te_4$ [28], and in a-$Gd_x Si_{1-x}$ samples [29]. We are not aware of any 3D system that was tested over a wide temperature range near its MIT without showing the ambiguous $G(T)$ characterizing the T^* problem. This feature may be generic to 3D systems near their Anderson transition.

The phenomenology associated with this anomalous $G(T)$, in particular the systematic increase of T^* with disorder and the absence of the effect in two dimensions [24], raised the possibility that T^* signifies the mobility edge, a threshold energy E_C separating extended states for $E > E_C$ from localized states for $E < E_C$. This indeed might account for the experimental observations. However, the values for T^* necessary for this line of explanation turned out to be smaller than what one (perhaps naively) anticipates. Note that near the metal-insulator transition the distance δE to the mobility edge is expected to obey [30]

$$\Delta E \equiv |E_C - E_F| = E^*|(g - g_c)/g_c|^\nu, \tag{5}$$

where E_F is the Fermi energy, g is the dimensionless conductance, g_c is the dimensional conductance value at the MIT transition, and the exponent ν is ≈ 1. To fit the $G(T)$ data to Eq. (5) it was necessary to use for E^* a value considerably smaller than the Fermi energy of the material, which shed some doubts on the notion that T^* reflects the mobility edge [24].

The current results, and in particular the apparent role of dimensionality, instigated a renewed look at these phenomena. The absorption experiments (Fig. 7) and the $G(T)$ behavior of just insulating 3D samples have this in common: Both exhibit diffusive characteristics, a tendency that becomes more conspicuous as they further approach the MIT, and both involve probing the system away from its ground state: The stress experiments take the system far from equilibrium, the T^* problem is a finite temperature phenomenon. Indeed, a simple explanation of the $G(T)$ anomaly might be related to a temperature-dependent probing length. An insulating sample will exhibit a diffusive $G(T)$ law when, for example, $L_{in} < \xi$ where $L_{in} = L_{in}(T)$ is the inelastic diffusion length. This however cannot account for the experimental T^* problem unless one assumes either an unusual energy dependence for ξ or a specific ξ distribution [31]. A many-body scenario may have to be considered.

Let us examine the T^* problem in the context of the current issue assuming for the moment it is in fact a mobility edge. If E_C is not far above E_F, then new avenues for electron-electron energy exchange may become available. It is thus of interest to find out how close is a system with a given $k_F\ell$ to the transition. This may be estimated from the dependence of the localization length ξ on the order parameter $k_F\ell$ of the sample in question. The localization length is evaluated using the $G(T)$ data with Eq. (4); this yields the $\xi(k_F\ell)$ plot shown in Fig. 9.

The dependence of ξ on $k_F\ell$ in this figure fits reasonably well the expression $\xi = \frac{\xi_0}{(k_F\ell)_C}[1 - \frac{k_F\ell}{(k_F\ell)_C}]^{-1}$ which is a variation on the scaling form [30] (with $\nu = 1$)

$$\xi = \xi_0|(g - g_c)/g_c|^{-\nu}, \tag{6a}$$

where ξ_0 is the value of the localization length far from the MIT. Fitting the dependence of ξ on $k_F\ell$ (Fig. 9) yields

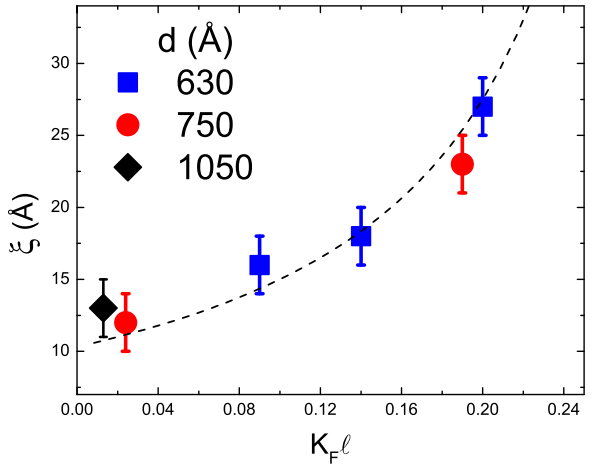

FIG. 9. (Color online) The dependence of the localization length ξ on the Ioffe-Regel parameter $k_F\ell$ for several of the studied films.

$\xi_0 = 11$ Å, which is of the order of the Bohr radius, $a_B \simeq 15$ Å for indium-oxide, so this is a plausible result. From Eqs. (6a) and (5) one gets

$$\Delta E = E^*(\xi_0/\xi) \tag{6b}$$

that can now be used for an estimate of E^*. Using Eq. (6b) with $\delta E \simeq 60$ K for the sample with $k_F\ell = 0.19$; $\xi = 23$ Å (see Fig. 9) gives $E^* \approx 120$ K. Note that, similar to the low values for E^*/E_F obtained in Ref. [24] for other systems, the current E^* is smaller by more than an order of magnitude than the Fermi energy of the material (E_F for In_xO with a carrier concentration $n = 8.1 \times 10^{19}$ cm^{-3} is $\simeq$1600 K).

This value for E^* yields $\delta E \simeq 50$ K for the sample with $k_F\ell = 0.21$; $\xi = 27$ Å which exhibits diffusivelike absorption characteristics when measured at $\approx$4 K. This does not contradict the observation of an insulating $G(T)$ behavior at this temperature range; thermal excitation to states lying $\approx$50 K above the mobility edge will only contribute significantly to the conductance exceeding $\approx$12 K. Note however that the distance to the mobility edge associated with $\Delta E \simeq 50$ K is not yet small enough to allow appreciable electron-electron energy exchange via virtual transitions to extended states; the time allowed for diffusion in these states $\hbar/\delta E$ is $\approx 10^{-13}$ s which is an order of magnitude shorter than $\gamma_{in}^{e\text{-}e}$ of the diffusive system at these temperatures [5,7]. It is therefore hard to see how to account for the results in Fig. 7 with a single-particle scenario and with just the implicit assumptions of system homogeneity made above.

For example one may consider the possibility that a significant part of the current-carrying path is composed of regions that are diffusive (and their combined resistance is comparable to that of the bottleneck resistors). The occurrence of "metallic puddles" within the globally insulating system is a likely scenario when the system approaches the metal-insulator transition from the insulating side [32]. This could be a consequence of the distributed nature of the localization length, a complication that is sometimes ignored on the (misguided) logic that a specific value for ξ is singled out by percolation constraints [33]. One should not be surprised to find deviations from the predictions of these models even for some aspects of the dc conductivity [34] and anyway, for measurements that involve the bulk of the sample, a realistic distribution of localization lengths should be taken into account. At finite frequencies diffusive regions need not percolate in the system; it is only necessary that the applied F_{stress} induces dissipative currents in them thus generating phonons in excess of those present in equilibrium. This then will be effective in system randomization with the ensuing (once Ohmic conditions are restored), slowly relaxing excess conductance which contributes to the perceived absorption.

A pertinent consideration here is a conceivable modification of the wave functions due to correlation and many-body effects. The Coulomb interaction on a scale of ξ derived from the $G(T)$ data is comparable with δE of the samples in Fig. 7 therefore hybridization with states above E_C cannot be ruled out [35]. It is difficult to estimate the relevance of these processes nearer the transition where the contribution of electronic polarization to the dielectric constant becomes dominant [36], so a self-consistent treatment must be invoked.

Another complication is that the states above E_C are actually localized in the ground state; they just *appear* to be extended under finite temperature or non-Ohmic fields (at high frequencies the latter will be effective even when the associated conductance change is smaller than that required by T due to the relative freedom from percolation constraints). Note that the many-body density of states grows extremely fast with energy (unlike in a single-particle scenario where this change is algebraic), and delocalization or an increase of the localization length [37] may occur due to the excess energy supplied by the stress field.

The combination of potential fluctuations, higher-order excitations, and extended states lying close to the Fermi energy may enhance the occurrence of metallic "puddles." Obviously, dimensionality plays a role in any of these scenarios. If however the observed E_C is a many-body mobility edge it should also occur in 2D systems albeit probably at a considerably higher energy. More experiments are needed to elucidate the relative importance of these mechanisms. The appearance of the T^* problem in so many systems may be suggestive of an underlying physical effect relevant for the MIT problem. It clearly deserves to be addressed whether it signifies a real mobility edge or it is just a consequence of a finite temperature measurement. The effectively low value of E^* (relative to E_F) means that, over a wide range of the physical parameters that are used to characterize the disorder, the system may be still within the "critical" regime of the metal-insulator transition.

E. Summary

We have presented results of energy absorption from applied electromagnetic fields in three-dimensional In_xO samples. For Anderson-insulating samples that are far from the metal-insulator transition, the absorption appears to be limited to frequencies that are of the order of the electron-phonon scattering rates of the material. This suggests that the hopping process in the range of temperature and disorder studied is mediated by phonons. Likewise, thermalization of the electronic system then hinges on the presence of a phonon bath. This is in agreement with the conclusions reached by

Fleishman and Anderson [1]. These authors also anticipated a change of behavior as the mobility edge is approached from below and expected that this would be reflected in $G(T)$ that ought to include contribution from activation to extended states. The experimentally observed change in $G(T)$ as the mobility edge is approached appears to be more complicated, and it would appear that more elaborate models of conductivity need to be developed for the critical transport regime. These may also shed light on the observation that absorption from ac fields is more sensitive than temperature to the proximity of a mobility edge (whether real or apparent).

The effective range of the interaction, clearly important to these issues, was not explicitly dealt with in our experiments. At finite temperatures the range of the Coulomb interaction is limited by the finite conductivity for which the relevant scale is presumably the hopping length $r(T)$. At liquid-helium temperatures and for the range of the disorder in the samples used in this study, $r(T)$ is of order of few hundred Å. This is an order of magnitude larger than the intercarrier separation $n^{-1/3}$ suggesting that, for the more disordered samples, our experimental results are relevant for systems with long-range interaction.

As the disorder in our samples was reduced and the diffusive phase approached, the absorption extended to progressively higher frequencies. This was observed in 3D samples but not in 2D samples with comparable degree of disorder. The similarity of this observation with the T^* problem that appears to be a common feature in many 3D systems near their MIT was pointed out. It is hoped that this problem will receive due theoretical attention. Possible relevance of a nearby mobility edge for bringing about this behavior as well as the diffusivelike absorption characteristics of just insulating 3D samples was discussed. Various effects that might contribute to these phenomena were mentioned including possible many-body effects. It would be interesting to extend the absorption study to include the dependence of the absorption on the amplitude of the stress field near the transition as it may shed some light on the relative importance of many-body effects.

ACKNOWLEDGMENT

This research has been supported by a grant administered by the Israel Academy for Sciences and Humanities.

[1] L. Fleishman and P. W. Anderson, Phys. Rev. B **21**, 2366 (1980).
[2] A. Mittal, *Quantum Transport in Submicron Structures*, Advanced NATO Proceedings (Kluwer Academic, Dordrecht, 1996).
[3] G. Bergmann, Phys. Rep. **107**, 1 (1984); S. Kobayashi and F. Komori, Prog. Theor. Phys. Suppl. **84**, 224 (1985).
[4] Z. Ovadyahu, Waves Random Media **9**, 241 (1999), and references therein.
[5] Z. Ovadyahu, Phys. Rev. Lett. **108**, 156602 (2012).
[6] J. H. Davies, P. A. Lee, and T. M. Rice, Phys. Rev. Lett **49**, 758 (1982); M. Grünewald *et al.*, J. Phys. C **15**, L1153 (1982); M. Pollak and M. Ortuño, Sol. Energy Mater. **8**, 81 (1982); M. Pollak, Philos. Mag. B **50**, 265 (1984); G. Vignale, Phys. Rev. B **36**, 8192 (1987); M. Müller and L. B. Ioffe, Phys. Rev. Lett. **93**, 256403 (2004); C. C. Yu, *ibid.* **82**, 4074 (1999); V. Malik and D. Kumar, Phys. Rev. B **69**, 153103 (2004); D. R. Grempel, Europhys. Lett. **66**, 854 (2004); E. Lebanon and M. Müller, Phys. Rev. B **72**, 174202 (2005); A. Amir, Y. Oreg, and Y. Imry, Annu. Rev. Condens. Matter Phys. **2**, 235 (2011); J. Bergli and Y. M. Galperin, Phys. Rev. B **85**, 214202 (2012); for a recent review and relevant literature see M. Pollak, M. Ortuño, and A. Frydman, *The Electron Glass* (Cambridge University Press, Cambridge, England, 2013).
[7] U. Givan and Z. Ovadyahu, Phys. Rev. B **86**, 165101 (2012).
[8] A. Vaknin, Z. Ovadyahu, and M. Pollak, Phys. Rev. B **65**, 134208 (2002).
[9] V. Orlyanchik and Z. Ovadyahu, Phys. Rev. Lett. **92**, 066801 (2004).
[10] A. Vaknin, Z. Ovadyahu, and M. Pollak, Phys. Rev. B **61**, 6692 (2000); A. Amir, Y. Oreg, and Y. Imry, Proc. Natl. Acad. Sci. USA **109**, 1850 (2012); Y. Meroz, Y. Oreg, and Y. Imry, Europhys. Lett. **105**, 37010 (2014).
[11] Z. Ovadyahu, Phys. Rev. B **73**, 214208 (2006).
[12] S. Marnieros, L. Bergé, A. Juillard, and L. Dumoulin, Phys. Rev. Lett. **84**, 2469 (2000).
[13] R. M. Hill, Philos. Mag. **24**, 1307 (1971); B. I. Shklovskii, Sov. Phys. Semicond. **6**, 1964 (1973) [Fiz. Tekh. Poluprovodn. **6**, 2335 (1972)]; R. M. Hill, Sov. Phys. Semicond. **10**, 855 (1976) [Fiz. Tekh. Poluprovodn. **10**, 1440 (1976)]; M. Pollak and I. Riess, J. Phys. C **9**, 2339 (1976).
[14] Z. Ovadyahu, Phys. Rev. B **84**, 165209 (2011).
[15] P. M. Echternach, M. R. Thoman, C. M. Gould, and H. M. Bozler, Phys. Rev. B **46**, 10339 (1992); M. E. Gershenson, D. Gong, T. Sato, B. S. Karasik, and A. V. Sergeev, Appl. Phys. Lett. **79**, 2049 (2001); A. Sergeev and V. Mitin, Europhys. Lett. **51**, 641 (2000).
[16] F. P. Milliken and Z. Ovadyahu, Phys. Rev. Lett. **65**, 911 (1990).
[17] A. Sergeev and V. Mitin, Phys. Rev. B **61**, 6041 (2000).
[18] S. Wessel, B. Normand, M. Sigrist, and S. Haas, Phys. Rev. Lett. **86**, 1086 (2001); H. G. Schlager and H. v. Löhneysen, Europhys. Lett. **40**, 661 (1997).
[19] O. Faran and Z. Ovadyahu, Phys. Rev. B **38**, 5457 (1988).
[20] I. V. Gornyi, A. D. Mirlin, and D. G. Polyakov, Phys. Rev. Lett. **95**, 206603 (2005); D. M. Basko, I. L. Aleiner, and B. L. Altshuler, Ann. Phys. (NY) **321**, 1126 (2006).
[21] V. Oganesyan and D. A. Huse, Phys. Rev. B **75**, 155111 (2007); R. Nandkishore, S. Gopalakrishnan, and D. A. Huse, *ibid.* **90**, 064203 (2014).
[22] N. F. Mott and A. E. Davis, *Electronic Processes in Non-Crystalline Materials* (Oxford University, New York, 1971).
[23] K. Ellmer and R. Mientus, Thin Solid Films **516**, 4620 (2008).
[24] Z. Ovadyahu, J. Phys. C: Solid State Phys. **19**, 5187 (1986).
[25] L. Zeng, E. Helgren, M. Rahimi, F. Hellman, R. Islam, B. J. Wilkens, R. J. Culbertson, and D. J. Smith, Phys. Rev. B **77**, 073306 (2008).
[26] A. Möbius, H. Vinzelberg, C. Gladun, A. Heinrich, D. Elefant, J. Schumann, and G. Zies, J. Phys. C: Solid State Phys. **18**, 3337 (1985).

[27] R. L. Rosenbaum, M. Slutzky, A. Möbius, and D. S. McLachlan, J. Phys.: Condens. Matter **6**, 7977 (1994); G. Eytan, E. Zaken, R. Rosenbaum, D. S. McLachlan, and A. Albers, Physica B **194-196**, 2419 (1994).

[28] T. Siegrist, P. Jost, H. Volker, M. Woda, P. Merkelbach, C. Schlockermann, and M. Wüttig, Nat. Mater. **10**, 202 (2011).

[29] P. Xiong, B. L. Zink, S. I. Applebaum, F. Hellman, and R. C. Dynes, Phys. Rev. B **59**, R3929 (1999).

[30] E. Abrahams, P. W. Anderson, D. C. Licciardello, and T. V. Ramakrishnan, Phys. Rev. Lett. **42**, 673 (1979).

[31] An example of a possible scenario that formally accounts for the T^* problem is based on assuming *two* distinct localization lengths ξ_1 and $\xi_2 > \xi_1$. Then insulating behavior will prevail at $T < T^*$ defined by $L_{\rm in}(T^*) > \xi_2$ and an insulating behavior with a parallel "metallic" conductance at $T > T^*$ [when $\xi_1 < L_{\rm in}(T) < \xi_2$].

[32] M. H. Cohen and J. Jortner, Phys. Rev. Lett. **30**, 699 (1973).

[33] B. I. Shklovskii and A. L. Efros, Zh. Eksp. Teor. Fiz. **60**, 867 (1971) [Sov. Phys. JETP **33**, 468 (1971)]; B. I. Shklovskii, Zh. Eksp. Teor. Fiz. **61**, 2 (1971) [Sov. Phys. JETP **34**, 1084 (1972)]; V. Ambegaokar, B. I. Halperin, and J. S. Langer, Phys. Rev. B **4**, 2612 (1971); M. Pollak, J. Non-Cryst. Solids **11**, 1 (1972).

[34] M. H. Brodsky, and R. J. Gambino, J. Non-Cryst. Solids **8-10**, 739 (1972).

[35] J. M. Bigelow and J. P. Leburton, Appl. Phys. Lett. **57**, 795 (1990).

[36] T. G. Castner, Phys. Rev. B **61**, 16596 (2000), and references therein.

[37] R. Berkovits, Phys. Rev. B **89**, 205137 (2014).